

Article

A Mathematical Model for Predicting the Droplet Size of Micro-Fog Nozzle with Circular-Hole Rotating Core Based on Orthogonal Design

Yan Cui ^{1,2}, Chuan Cheng ¹, Pengfei Wang ^{1,2,*}, Yong Liu ^{1,2}, Runqiu Li ¹, Yong Zhang ¹ , Ming Li ³ 
and Shilin Li ¹

¹ School of Resource, Environment & Safety Engineering, Hunan University of Science & Technology, Xiangtan 411201, China

² Work Safety Key Lab on Prevention and Control of Gas and Roof Disasters for Southern Coal Mines, Hunan University of Science & Technology, Xiangtan 411201, China

³ School of Resource & Safety Engineering, Central South University, Changsha 410083, China

* Correspondence: pfwang@sina.cn

Abstract: The circular-hole rotating core fog nozzle has excellent atomization performance and has been widely used in the realm of spray dust. As part of this study, a mathematical model was developed for predicting the Sauter mean diameter (SMD) of nozzles of this type. The coaction between the SMD of the nozzle and the three influencing factors of axial distance, water supply pressure, and outlet diameter was investigated based on the customized spray's experimental platform and orthogonal design method. According to the comparative analysis of the size range, the axial distance, outlet diameter and water supply pressure are three parameters that affect the SMD of the nozzle, and the degree of influence is axial distance > outlet diameter > water supply pressure. On this basis, a mathematical model was developed using the multiple regression method to predict the SMD of the nozzle. We analyzed the results and compared them to the SMD value predicted by the multiple regression mathematical model and the orthogonal experiment results. The change trend was the same, the values were essentially the same, and the average relative error was just 16.11%. Accordingly, the mathematical model presented in this paper may be used for the prediction and calculation of the droplet size for circular-hole rotating core micro-fog nozzles.

Keywords: nozzle droplet size; orthogonal design; regression analysis; SPSS software; mathematical model



Citation: Cui, Y.; Cheng, C.; Wang, P.; Liu, Y.; Li, R.; Zhang, Y.; Li, M.; Li, S. A Mathematical Model for Predicting the Droplet Size of Micro-Fog Nozzle with Circular-Hole Rotating Core Based on Orthogonal Design. *Appl. Sci.* **2023**, *13*, 6670. <https://doi.org/10.3390/app13116670>

Academic Editor: Dino Musmarra

Received: 19 March 2023

Revised: 27 April 2023

Accepted: 26 May 2023

Published: 30 May 2023



Copyright: © 2023 by the authors. Licensee MDPI, Basel, Switzerland. This article is an open access article distributed under the terms and conditions of the Creative Commons Attribution (CC BY) license (<https://creativecommons.org/licenses/by/4.0/>).

1. Introduction

Production activities such as mining and metal smelting produce a large amount of dust, and the health and safety of workers exposed to high concentrations of dust for a long time will face serious risks [1–4], especially from PM_{2.5} (particles with aerodynamic diameters of $\leq 2.5 \mu\text{m}$) [5–10]. The main dust control measures are ventilation, vacuum cleaner dust purification, spray dust suppression, fence dust, etc. [11,12]. Nowadays, the primary technology that deals with dust pollution domestically and abroad is spraying. The atomizing nozzle is an important accessory in spraying [13–17]. Among various nozzle types, the pressure-atomizing nozzle is the most widely used because of its simple structure and strong adaptability. Due to its simple structure and strong adaptability, pressure atomizing nozzle has become the most widely used nozzle [18–23]. The principle is that the liquid is transported to the nozzle port by liquid pressure or gas pressure, mixed in the liquid cap of the pressure-atomizing nozzle, and then sprayed through the nozzle hole of the pressure-atomizing nozzle [24,25]. Among them, the circular-hole rotating core micro-fog nozzle is widely used in fog gun vehicles. Compared with normal pressure atomization, the strengths of the circular-hole rotating core micro-fog nozzle include its low

water pressure requirements, low water consumption, and high dust removal efficiency (especially for respirable dust). However, this nozzle is seldom studied at present. A number of scholars have conducted extensive experiments and numerical simulations to discuss the impact factors of droplet size, such as nozzle types, water supply pressure, and the distance between the measurement point and the spray nozzle. Kozo Saito et al. used the integral form of the conservation equation to establish a system of equations that can be solved to analyze far-field secondary atomization by predicting the droplet size and velocity distribution of the relevant phases [26]. P. E. Sojka et al. proposed a theoretical model to combine internal flow dynamics to better predict the deformation of droplets and the resulting breakup in a continuous, uniform air jet under multi-mode breakup conditions [27]. Carlos A. Renaudo proposed a new model to represent the atomization of pre-hole nozzles [28]. K. Lachin performed a rigorous dimensional analysis of the two-fluid spray characteristics [29]. In China, Liu et al. established the droplet size distribution equation of a swirl nozzle by creating a mathematical model [30–32]. Qu et al. established a mathematical model of nozzle atomization characteristics and the average droplet diameter and analyzed it [33,34].

Previously, scholars have focused on one factor to determine droplet size in their studies, and the ultrasonic nozzle with a liquid medium was thoroughly studied for its atomization mechanism; however, there were few studies on the degree of influence of different factors on droplet size and the correlation between the main influencing factors and droplet size. At the same time, it has been reported that some scholars have investigated the droplet size produced by this type of nozzle and have developed a simple mathematical model to predict the droplet size. Nevertheless, the existing mathematical models did not take into account all the factors affecting droplet size. Due to this, the established droplet prediction model cannot be applied to the development of programs at engineering sites. Based on the different parameters of the three nozzles and the customized spraying experimental platform, the SMD (the Sauter Mean Diameter) of three different outlet diameters of round-hole rotating core micro-mist nozzles under three different water supply pressures and three different axial distances were measured. The SMD change of the nozzle was studied by the orthogonal experimental design method to fill the gap in the relationship between the outlet diameter, water supply pressure, and axial distance in the existing research. Finally, based on the above, the mathematical model of the SMD was established by using the multiple regression method, which provides a powerful tool for the parameter prediction of the round-hole rotating core micro-mist nozzle.

2. Experimental System and Scheme

2.1. Experimental System

As shown in Figure 1, the experimental platform for the circular-hole rotating core micro-fog nozzle was composed of a water tank, pump, control cabinet, flow meter frequency converter, digital manometer, a Malvern real-time high-speed spray particle size analyzer, and related pipes and valves. A frequency converter was used to adjust the pump's output water pressure. The water supply pressure was measured by a digital manometer, while the water flow rate was measured by a flow meter. Real-time monitoring of the droplet size distribution in the droplet field was conducted with a high-speed spray particle size analyzer. The experimental site is shown in Figure 2.

In this paper, the circular-hole rotating core micro-fog nozzle was made of stainless steel coated with a layer of chromium. The water supply port and the connecting pump outlet specifications were unified as 0.5 feet external thread. The nozzle outlet diameter had three specifications: 0.5 mm, 0.7 mm, and 1.1 mm. The nozzle shape and structure are shown in Figure 3.

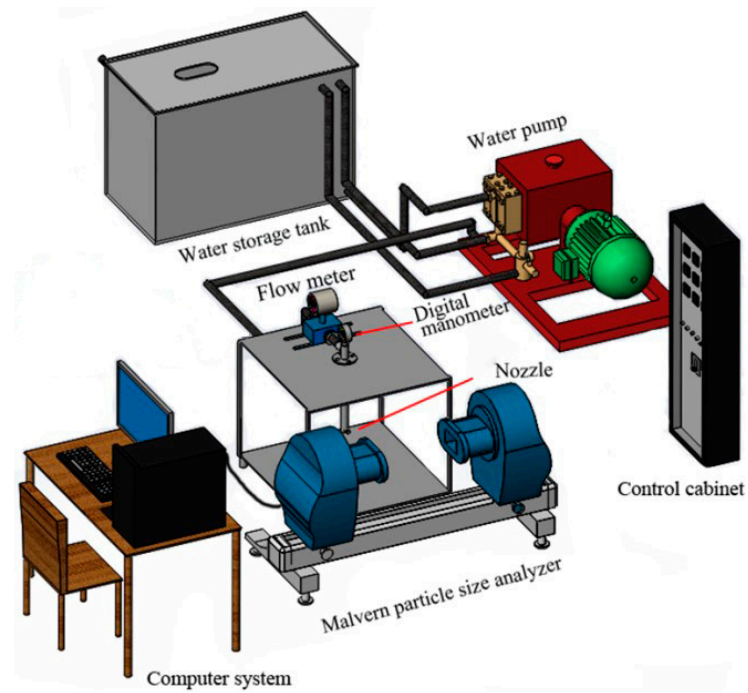


Figure 1. Experimental system.



Figure 2. Experimental site: (a) Malvern particle size analyzer; (b) computer system; (c) control cabinet.

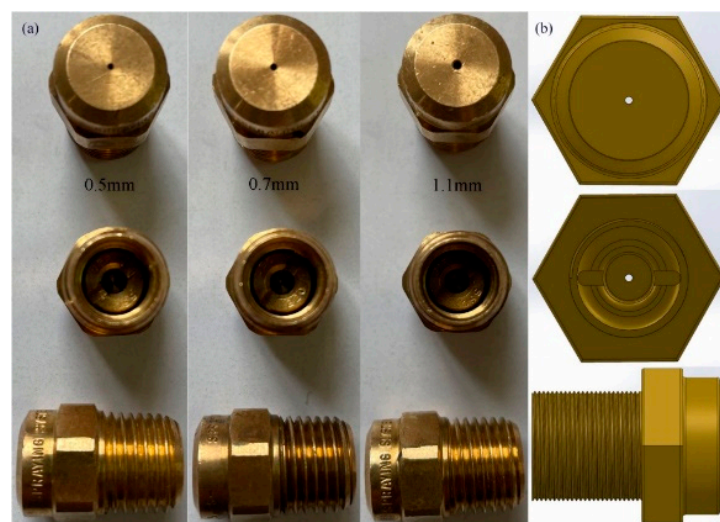


Figure 3. The test used a circular-hole rotating core micro-fog nozzle and structure: (a) nozzle shape; (b) 0.7 mm nozzle structure diagram.

2.2. Experimental Scheme

The droplet size and particle size distribution were measured by the Malvern particle size analyzer after atomization. The types of outlet diameters were 0.5 mm, 0.7 mm, and 1.1 mm, and the water supply pressure was adjusted to 1.0 MPa, 2.0 MPa, and 3.0 MPa by adjusting the frequency of the pump. The droplet size at 50 cm and 70 cm from the nozzle outlet was measured according to the same procedure, and a total of 27 sets of experimental data were obtained.

This study analyzed the ultrasonic atomization nozzle's atomization performance using the orthogonal design method. Multiple levels and factors can be analyzed using an orthogonal experimental design by using the fewest number of tests, and equivalent results can be achieved for a large number of comprehensive trials. Before performing the orthogonal experiments, we determined the protocol using orthogonal tables [18].

The droplet size of the circular-hole rotating core micro-fog nozzle was studied by orthogonal experiments. For the circular-hole rotating core micro-fog nozzle, the axial distance (S), the outlet diameter (D), and the water supply pressure (P) are the factors that affect the atomization parameters. Therefore, the axial distance (S), the outlet diameter (D), and the water supply pressure (P) were taken as the three influencing factors of the orthogonal design. Each factor was set at three levels, and the orthogonal design method of the "three factors and three levels" was used for the research; the factor levels are shown in Table 1. The results of the orthogonal experiments are shown in Table 1.

Table 1. Factors and levels in the orthogonal experimental.

Serial Number	S (cm)	D (mm)	P (MPa)
1	30	0.5	1
2	50	0.7	2
3	70	1.1	3

3. Experimental Results and Analysis

3.1. Droplet Size Parameter Analysis

Table 2 show the droplet size parameters of the circular-hole rotating core micro-fog nozzle under different Ps and different Ss. It can be seen from the droplet size parameters of the atomizing nozzle in Table 1 that when the D was increased, the droplet characteristic particle size and the average particle size were reduced. $D_{[3,2]}$ and $D_{[4,3]}$ represent the Sauter mean diameter (SMD) and the volume-weighted mean diameter, respectively; D_{50} is the characteristic particle size, representing a particle volume of less than 50% of the total volume of all the particles. The units are in μm .

For example, when the S was 30 cm, the P was 1 MPa, and the D was increased from 0.5 mm to 1.1 mm, the $D_{[3,2]}$ was reduced from 516.1 μm to 274.6 μm , and the D_{50} was reduced from 681.3 μm to 672.5 μm ; when the S increased, the D_{50} and $D_{[3,2]}$ also decreased with the increase of the axial distance. For example, when the D was 0.5 mm, the P was 1 MPa, and the S increased from 30 cm to 70 cm, the $D_{[3,2]}$ decreased from 516.1 μm to 87.5 μm , and the D_{50} decreased from 681.3 μm to 110.2 μm ; both the D_{50} and $D_{[3,2]}$ decreased with the increasing P. For example, when the D was 30 cm, the S was 0.5 mm, and the P increased from 1 MPa to 3 MPa, the $D_{[3,2]}$ decreased from 516.1 μm to 208.1 μm , and the D_{50} decreased from 681.3 μm to 674.6 μm . Thus, it can be seen the influence of the S on the nozzle droplet size was much greater than the other two factors. In addition, when the S was 50 cm, both the D_{50} and $D_{[3,2]}$ decreased sharply, whether by increasing the D or the P, and the decrease was particularly pronounced when the D was increased. To obtain liquid droplet size with better dust removal efficiency, that was, $D_{[3,2]} < 90 \mu\text{m}$, the pressure of a typical pressure atomizing nozzle needs to be adjusted to above 6 MPa. In contrast, the $D_{[3,2]}$ was less than 90 μm when the circular-hole rotating core micro-fog nozzle was 3 MPa, which can be applied to some places with low water pressure.

Table 2. Droplet size parameters.

S/cm	D/mm	P/MPa	D ₅₀	D _[3,2]	D _[4,3]	S/cm	D/mm	P/MPa	D ₅₀	D _[3,2]	D _[4,3]
30	0.5	1	681.3	516.1	677.2	70					
	0.5	2	681.5	567.9	681.0						
	0.5	3	674.6	208.1	580.3						
	0.7	1	668.4	212.4	534.2						
	0.7	2	668.8	201.3	536.2						
	0.7	3	658.2	160.5	482.8						
	1.1	1	672.5	274.6	571.0						
	1.1	2	668.1	238.6	533.3						
	1.1	3	656.1	199.8	474.5						
	0.5	1	669.5	321.5	553.5						
	0.5	2	544.8	191.8	468.0						
	0.5	3	296.0	111.3	349.8						
	0.7	1	139.1	99.0	333.8						
	0.7	2	80.3	58.3	152.2						
0.7	3	71.4	57.5	192.1							
50	1.1	1	95.0	64.4	153.0						
	1.1	2	81.2	54.5	90.4						
	1.1	3	84.9	64.7	165.4						
	0.7	1	110.2	87.5	155.5						
	0.5	1	105.9	86.2	238.1						
	0.5	2	93.7	70.8	331.7						
	0.7	1	62.0	47.0	160.6						
	0.7	2	61.5	49.1	144.2						
	0.7	3	71.8	60.2	230.4						
	1.1	1	68.2	51.9	77.3						
	1.1	2	64.7	50.2	72.9						
	1.1	3	71.9	53.5	101.4						

3.2. Droplet Size Distribution Analysis

The $D_{[3,2]}$ of the circular-hole rotating core micro-fog nozzle was almost below 90 μm when the axial distance was 70 cm, and the droplet size data were very ideal. Therefore, in this section, we selected the droplet size distribution with an axial distance of 70 cm for analysis. There is the droplet size distribution of the circular-hole rotating core micro-fog nozzle under different Ps and different Ds at an S of 70 cm in Figure 4. As can be seen from the cumulative volume fraction curve in Figure 4, the P is fixed, the nozzle outlet pipe diameter is increased, the $D_{[3,2]}$ has a little fluctuation, and the overall performance is gradually increasing; when the D was constant, the $D_{[3,2]}$ decreased with the increase of the P. As can be seen from Figure 4, the P is fixed, and with the increase of D, the droplet volume frequency peak moves to the right, that is, toward the direction of the increasing droplet particle content; at the same time, it can be seen from the histogram of the capacity frequency spectrum that with the increase of the P, the peak value of the capacity frequency spectrum showed a trend of increasing continuously and then decreasing slowly. Figure 4 is a volume frequency histogram, from which we can also see that when the D was constant, as the pressure of the water supply increased, the droplet size distribution range was smaller than before, and the peak value increased first and then decreased. When the P was constant, with the D increased, the droplet size distribution range became larger, and the peak gradually increased.

As we can see, the SMD generally conforms to the normal distribution from Figure 4. When the D remains unchanged, the atomization ability will gradually increase with the enlargement of the P. The enhancement of the atomization ability will help to prevent the breakup of the droplets, resulting in a decrease in droplet size. Keeping the nozzle water supply pressure unchanged and reducing the nozzle outlet diameter, the Weber number of the liquid flow will become larger, which will lead to the increase of the surface disturbance amplitude of the water jet emitted by the nozzle, making the atomization effect of the nozzle more perfect and showing the regularity that the droplet size decreases with the decrease of the diameter of the outlet pipe. Similarly, the turbulence and cavitation generated by the internal structure of the nozzle affect the primary atomization of the jet ejected from the nozzle. When the outlet diameter was set to be small, the turbulence of the liquid in the nozzle would increase, and the local friction of the liquid would increase, resulting in more complete jet damage [35].

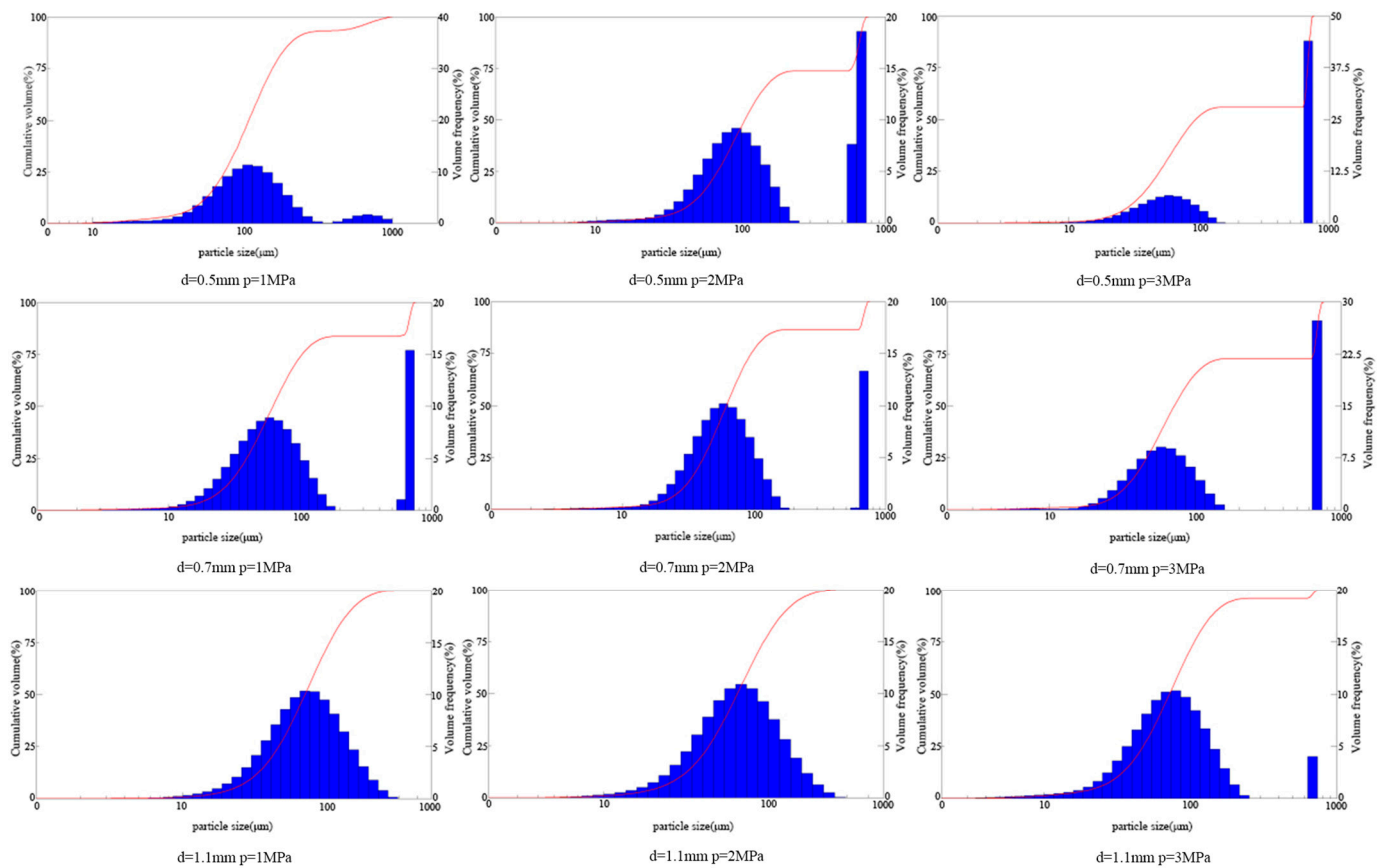


Figure 4. Droplet size distribution under different water supply pressures and outlet diameters at a 70 cm axial distance of the circular-hole rotating core micro-fog nozzle.

3.3. Droplet Size Analysis with Orthogonal Experiment

The orthogonal test results of the droplet size are shown in Table 3. In accordance with the orthogonal experiment theory, it was necessary to average the three factors in this paper at the same level to find the overall average of each factor at the same level. The MAX of each horizontal average of these three factors was subtracted from the minimum value, and the value range of each influencing factor was obtained. The large range indicates that the difference in the influencing factors was large. This factor was an important factor in the three factors; the small range showed that the difference of the influencing factors was small, and through the analysis of the range method, the primary and secondary influence of the various factors on the droplet size could be obtained. $D_{[3,2]}$ was the Sauter mean diameter (SMD), which could better reflect the droplet size. The droplet size analyzed in this section was $D_{[3,2]}$.

Table 3. Orthogonal experiment results.

Serial Number	S/cm	D/mm	P/MPa	D_{50}	$D_{[3,2]}$	$D_{[4,3]}$
1	30	0.5	1	681.3	516.1	677.2
2	30	0.7	3	658.2	160.5	482.8
3	30	1.1	2	668.1	238.6	533.3
4	50	0.5	3	296.0	111.3	349.8
5	50	0.7	2	80.3	58.3	152.2
6	50	1.1	1	98.0	64.4	153
7	70	0.5	2	105.9	86.2	238.1
8	70	0.7	1	62.0	47.0	160.6
9	70	1.1	3	71.9	53.5	101.4

Figure 5 shows the combined mean and range of the three factors. Through the range size comparison, it can be seen that of the three influencing factors, the axial distance had the greatest influence on the SMD, followed by the outlet diameter, and, finally, the water supply pressure. It can be seen from Figure 5a that when the S was 30 cm, the range of the SMD was 305.1 μm ; when the S was 50 cm, the range of the SMD was 78.0 μm ; when the S was 70 cm, the range of the SMD was 62.2 μm . Due to the increase of the S, the SMD gradually became smaller. The main reason was that the droplets with a smaller particle size could move farther because of the small air obstruction caused by their small size. It can be seen from Figure 5b that the range of the SMD decreased first and then increased with the increase of the D. As shown in Figure 5c, the SMD continued to decrease due to the increase of the P, but the increase continued to decrease. When the P increased from 1.0 MPa to 3.0 MPa, the SMD decreased from 209.2 μm to 127.7 μm and then to 108.4 μm . This was because when the pressure difference increased, the diameter of the gas core in the center of the nozzle would increase, resulting in the thinning of the liquid film. Therefore, under the influence of higher power and larger disturbance wave expansion on the surface, the liquid film was broken, resulting in the smaller droplet size.

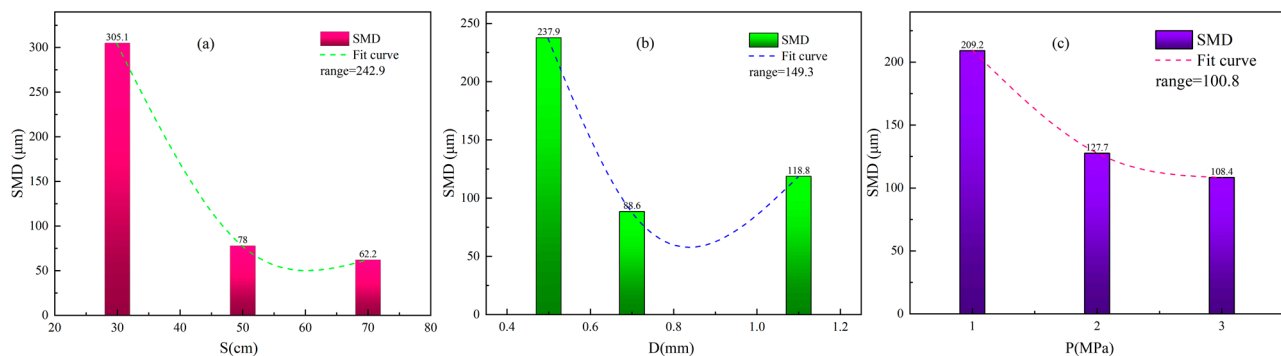


Figure 5. Comprehensive mean and range of three factors: (a) axial distance and SMD; (b) outlet diameter and SMD; (c) water supply pressure and SMD.

It can be seen from Figure 5 that the range was the smallest when the S was 70 cm, the range was the smallest when the S was 0.7 mm, and the range was the smallest when the P was 2 MPa. Therefore, an S of 70 cm, a D of 0.7 mm, and a P of 2 MPa was the best solution to improve the dust removal efficiency.

4. Regression Analysis and Model Verification

4.1. Regression Analysis

In order to determine the specific influence degree of the above three factors on the SMD of the circular-hole rotating core micro-fog nozzle, generally, high-order polynomials are used to predict the relationship between independent variables and dependent variables. However, the preliminary analysis of the data by Statistical Product and Service Solutions (SPSS) software (version 24.0.0.0) showed that if the ternary cubic polynomial was used for analysis, the principle of the consistent variance in the group could not be satisfied, and the so-called variance analysis could not be carried out at all. Therefore, the relationship between the droplet size, $D_{[3,2]}$, and the independent variable outlet diameter, (D), and the water supply pressure (P) and the axial distance (S) can be regarded as a ternary quadratic polynomial. According to the McLaughlin expansion, the multiple regression model was:

$$D_{[3,2]} = b_0 + b_1S + b_2D + b_3P + b_{11}S^2 + b_{22}D^2 + b_{33}P^2 + b_{12}SD + b_{13}SP + b_{23}DP \quad (1)$$

The overall significance test of the droplet size regression model by the SPSS multiple regression analysis is shown in Table 4, where R^2 is the determination coefficient and F is the statistical verification value.

Table 4. Global significance test of particle size regression model.

Variance Source	Freedom	F	p > F
Model	10	41.253	<0.001
Error	17		
Overall difference	27		R ² = 0.811 R ² (revise) = 0.802

As can be seen from Table 4, the coefficient of determination, R², of the regression model, with the introduction of the correction term in the established multiple regression model, was 0.802, which indicated that the degree of closeness between the dependent variate and the independent variate of the model was high and that the degree of explanation for the change of the dependent variable was described and explained by the multiple linear regression equation. The p of the overall significance test of the regression model was less than 0.001, which was far less than the set significance level of α = 0.05, and its significance had an obvious influence, which indicates that the overall regression model was very significant, and the hypothesis of the regression model was correct. The regression equation of the established multiple regression model was:

$$D_{[3,2]} = 2269.243 - 15.594S - 2342.524D - 216.007P + 0.193S^2 + 1314.13D^2 - 1.942P^2 + 0.955SD - 3.053SP + 21.15DP \tag{2}$$

4.2. Model Verification

The multiple regression model established by the above method could also approximately calculate the SMD prediction value of the circular-hole rotating core micro-fog nozzle, but the geometric correctness of the prediction value needed to be confirmed. For further testing the experimental correctness of the study on the prediction model results, the experimental values of the above 27 groups of the orthogonal models were taken for comparison with the predicted experimental values of the mathematical model, respectively, as a consequence. This is shown in Figure 6.

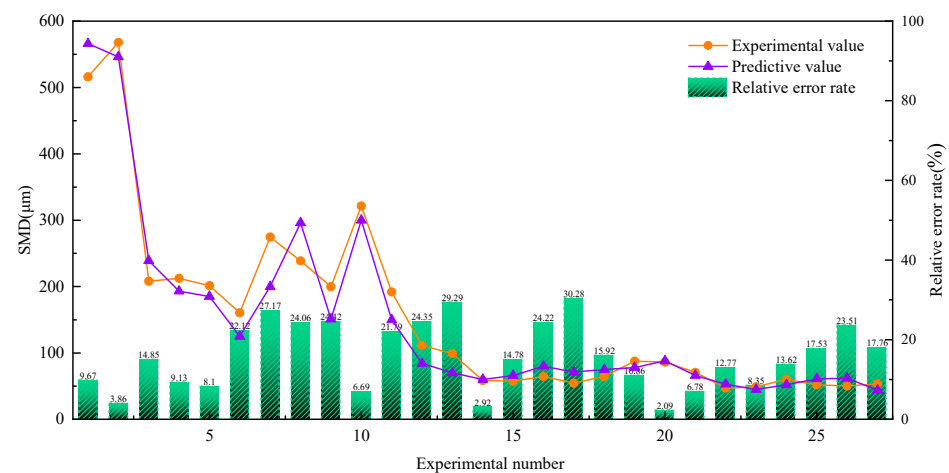


Figure 6. Comparison between SMD experimental value and predicted value.

From Figure 6, it can be seen the SMD prediction value of the multiple regression mathematical model was basically consistent with the change trend of the SMD value measured by the orthogonal experiment. The maximum relative error was 30.28%, the minimum was 2.09%, and the average relative error was 16.11%, less than 20%. It can be seen the model can precisely represent the relationship between the axial distance, outlet diameter, water supply pressure, and the SMD.

4.3. Nozzle Comparison

Compared with this paper, the nozzle in the literature [36] was an ultrasonic atomizing nozzle. The experimental platform used was the same as that in this paper. Multivariate nonlinear regression fitting was used to correct the average phase error of about 5%. By comparing Figure 7 with Figure 6, it can be concluded that the so-called ultrasonic atomizing nozzle used in the literature has a smaller droplet size under lower water pressure conditions, which is much better than the atomization performance of the circular-hole rotating core fog nozzle used in this paper. However, the use of an ultrasonic atomizing nozzle also needs to intake air at the inlet and further refine the droplets in the mixing chamber and the vibration chamber to obtain a better atomization effect. In contrast, the nozzle selected in this paper did not need air intake, which can meet the use of most conditions, and the atomization effect was satisfactory.

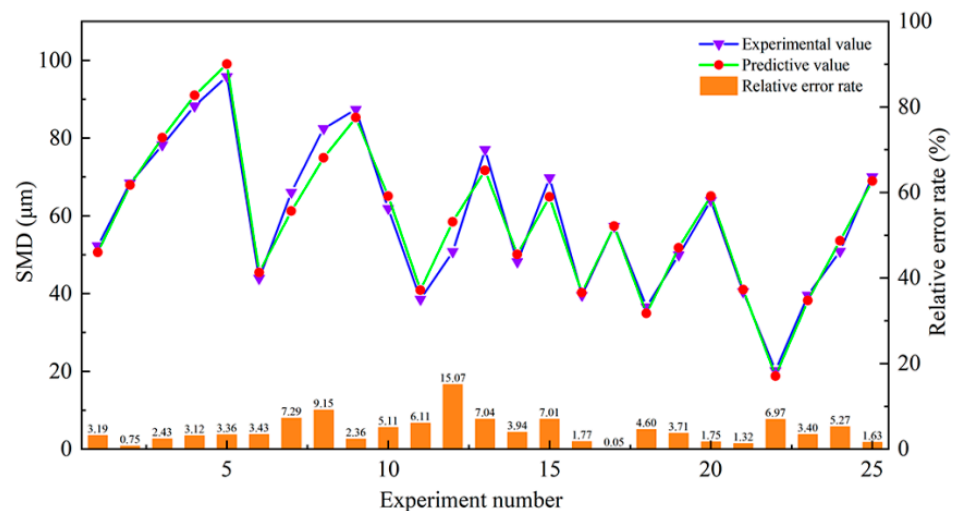


Figure 7. Comparison of experimental and predicted values of the SMD in the literature.

5. Conclusions

- (1) In this paper, the mathematical model for predicting the SMD of the circular-hole rotating core micro-fog nozzle was constructed and included the axial distance, outlet diameter, and water supply pressure. The droplet size decreased with the increase of the axial distance and water supply pressure. As the outlet diameter increased, the droplet size decreased first and then increased.
- (2) Through the analysis of the range method, it was concluded that among the three factors, the axial distance had the greatest influence on the droplet size, followed by the outlet diameter; the water supply pressure had the least influence on it.
- (3) According to Figure 5, the smaller the droplet size of the nozzle, the higher the ability to remove dust. In order to obtain the droplet size with the best dust removal effect, the optimal level of the factors was an outlet diameter of 1.1 mm, a water supply pressure of 1 MPa, and an axial distance of 70 cm.
- (4) The predicted value of the mathematical model for predicting the SMD of the circular-hole rotating core micro-fog nozzle was in basic agreement with the experimental value, and the average relative error was 16.11%, which was less than 20%.

Author Contributions: Conceptualization, Y.C. and C.C.; methodology, P.W.; software, C.C.; validation, Y.L., R.L. and Y.Z.; formal analysis, C.C.; writing—original draft preparation, C.C.; writing—review and editing, Y.C.; supervision, M.L.; project administration, S.L. All authors have read and agreed to the published version of the manuscript.

Funding: Financial support for this work was provided by the Natural Science Foundation of Hunan (2020JJ5172), the Scientific Research Project of the Hunan Province Office of Education

(No. 19B197), and the Science and Technology Innovation Project of the Hunan Provincial Department of Communications (201943).

Institutional Review Board Statement: Not applicable.

Informed Consent Statement: Not applicable.

Acknowledgments: Financial support for this work was provided by the Natural Science Foundation of Hunan (2020JJ5172), the Scientific Research Project of the Hunan Province Office of Education (No. 19B197), and the Science and Technology Innovation Project of the Hunan Provincial Department of Communications (201943), and they are gratefully acknowledged.

Conflicts of Interest: The authors declare no conflict of interest.

References

1. Cheng, W.M.; Zhou, G.; Chen, L.J. Research progress and prospect of dust control theory and technology in China's coal mines in the past 20 years. *Coal Sci. Technol.* **2020**, *48*, 1–20.
2. Bi, M.C.; Yao, J.; Yu, M. Characteristic features of dust blasts in the MOTAS/carbon black mixed system. *J. Saf. Environ.* **2017**, *17*, 169–173.
3. Yuan, L. Scientific conception of coal mine dust control and occupational safety. *J. China Coal Soc.* **2020**, *45*, 1–7.
4. Huang, Z.; Huang, Y.; Yang, Z.J.; Zhang, J.; Zhang, Y.H.; Gao, Y.K.; Shao, Z.L.; Zhang, L.H. Study on the physicochemical characteristics and dust suppression performance of new type chemical dust suppressant for copper mine pavement. *Environ. Sci. Pollut. Res.* **2021**, *28*, 59640–59651. [[CrossRef](#)]
5. Ma, X.Y.; Xiao, Z.H.; He, L.Z.; Cao, Y.J.; Liu, J.S. Comparison of chemical characteristics of PM_{2.5} during two winters in Xiangtan City in south central China. *J. Atmos. Chem.* **2020**, *77*, 169–183. [[CrossRef](#)]
6. Ma, X.Y.; Xiao, Z.H.; He, L.Z.; Shi, Z.B.; Cao, Y.J.; Tian, Z.; Tuan, V.; Liu, J.S. Chemical Composition and Source Apportionment of PM_{2.5} in Urban Areas of Xiangtan, Central South China. *Int. J. Environ. Res. Public Health* **2019**, *16*, 539. [[CrossRef](#)]
7. Yang, Z.C. Modeling and forecasting daily movement of ambient air mean PM_{2.5} concentration based on the elliptic orbit model with weekly quasi-periodic extension: A case study. *Environ. Sci. Pollut. Res.* **2014**, *21*, 9959–9972. [[CrossRef](#)]
8. Liu, Y.L.; Shi, S.L.; Wang, G.X.; Li, H.; Wang, T. Micro-particles stabilized aqueous foam for coal spontaneous combustion control and its flow characteristics. *Process Saf. Environ. Prot.* **2020**, *139*, 262–272. [[CrossRef](#)]
9. Jia, X.L.; Wu, J.K.; Lian, C.J.; Wang, J.J.; Rao, J.L.; Feng, R.J.; Chen, Y. Investigating the effect of coal particle size on spontaneous combustion and oxidation characteristics of coal. *Environ. Sci. Pollut. Res.* **2022**, *29*, 16113–16122. [[CrossRef](#)]
10. Huang, H.; Zhang, L.H.; Yang, Z.J.; Zhang, J.; Gao, Y.K.; Zhang, Y.H. Preparation and properties of a rock dust suppressant for a copper mine. *Atmos. Pollut. Res.* **2019**, *10*, 2010–2017. [[CrossRef](#)]
11. Hu, J.H.; Li, N.P.; Zou, S.H.; Hiroshi, Y.; Yanagi, U.; Yu, C.W.; Qu, H.D. Indoor environmental conditions in schoolchildren's homes in central-south China. *Indoor Built Environ.* **2020**, *29*, 956–971. [[CrossRef](#)]
12. Zhang, Z.Y.; Yin, W.; Wang, T.W.; O'Donovan, A. Effect of cross-ventilation channel in classrooms with interior corridor estimated by computational fluid dynamics. *Indoor Built Environ.* **2022**, *31*, 1047–1065. [[CrossRef](#)]
13. Wang, P.F.; Han, H.; Tian, C.; Liu, R.H.; Jiang, Y.D. Experimental study on dust reduction via spraying using surfactant solution. *Atmos. Pollut. Res.* **2020**, *11*, 32–42. [[CrossRef](#)]
14. Wang, P.F.; Shi, Y.J.; Zhang, L.Y.; Li, Y.J. Effect of structural parameters on atomization characteristics and dust reduction performance of internal-mixing air-assisted atomizer nozzle. *Process Saf. Environ. Prot.* **2019**, *128*, 316–328. [[CrossRef](#)]
15. Wang, P.F.; Tan, X.H.; Zhang, L.Y.; Li, Y.J.; Liu, R.H. Influence of particle diameter on the wettability of coal dust and the dust suppression efficiency via spraying. *Process Saf. Environ. Prot.* **2019**, *132*, 189–199. [[CrossRef](#)]
16. Wang, P.F.; Han, H.; Liu, R.H.; Gao, R.Z.; Wu, G.G. Effect of outlet diameter on atomization characteristics and dust reduction performance of X-swirl pressure nozzle. *Process Saf. Environ. Prot.* **2020**, *137*, 340–351. [[CrossRef](#)]
17. Wang, P.F.; Jiang, Y.D.; Liu, R.H.; Liu, L.M.; He, Y.C. Experimental Study on the Improvement of Wetting Performance of OP-10 Solution by Inorganic Salt Additives. *Atmos. Pollut. Res.* **2020**, *11*, 153–161. [[CrossRef](#)]
18. Wang, P.F.; Tian, C.; Liu, R.H.; Wang, J. Mathematical model for multivariate nonlinear prediction of SMD of X-type swirl pressure nozzles. *Process Saf. Environ. Prot.* **2019**, *125*, 228–237. [[CrossRef](#)]
19. Nie, W.; Liu, Y.H.; Cheng, W.M.; Zhou, G.; Ma, X. Dust removal technology of eject spraying between hydraulic supports on fully mechanized mining face. *J. Cent. South Univ. (Sci. Technol.)* **2015**, *46*, 4384–4390.
20. Gui, Z. *Experimental Study on the High Efficiency Spray and Dust Removal in Coal Mine*; Hunan University of Science and Technology: Xiangtan, China, 2017.
21. Ma, X. *Research on the Spray Atomization Law and Dust Reduction Technology in Fully Mechanized Coal Mining Face*; Shandong University of Science and Technology: Qingdao, China, 2017.
22. Cheng, W.M.; Liu, G.M.; Chen, L.J. Research Progress of Mine Shotcrete Dust Control Technology. *Saf. Coal Mines* **2020**, *51*, 87–97.
23. Wang, P.F.; Liu, R.H.; Wang, H.Q. Atomization characteristics of air-water spray in underground coal mine. *J. China Coal Soc.* **2017**, *42*, 1213–1220.

24. Zhang, Y.; Liu, S.Y.; Liu, Q.; Wang, X.; Jiang, Z.L.; Wei, J.F. The Role of Debris Cover in Catchment Runoff: A Case Study of the Hailuogou Catchment, South-Eastern Tibetan Plateau. *Water* **2019**, *11*, 2601. [[CrossRef](#)]
25. You, B.; Xu, J.X.; Shi, S.L.; Liu, H.Q.; Lu, Y.; Liang, X.Y. Treatment of Coal Mine Sewage by Catalytic Supercritical Water Oxidation. *Fresenius Environ. Bull.* **2020**, *29*, 497–502.
26. Poozesh, S.; Akafuah, N.K.; Campbell, H.R.; Bashiri, F.; Saito, K. Experimental and mathematical tools to predict droplet size and velocity distribution for a two-fluid nozzle. Campbell H R. *Fluids* **2020**, *5*, 231. [[CrossRef](#)]
27. Obenauf, D.G.; Sojka, P.E. Theoretical deformation modeling and drop size prediction in the multimode breakup regime. *Phys. Fluids* **2021**, *33*, 092113. [[CrossRef](#)]
28. Renaudo, C.A.; Yommi, A.; Slaboch, G.; Bucalá, V.; Bertin, D.E. Prediction of droplet size distributions from a pre-orifice nozzle using the Maximum Entropy Principle. *Chem. Eng. Res. Des.* **2022**, *185*, 198–209. [[CrossRef](#)]
29. Lachin, K.; Niane, M.; Person, M.; Mazet, J.; Delaplace, G.; Turchiuli, C. Prediction of droplets characteristic diameters and polydispersity index induced by a bifluid spraying nozzle by the means of dimensional analysis. *Chem. Eng. Sci.* **2023**, *265*, 118187. [[CrossRef](#)]
30. Liu, M.L.; Zhang, X. Research on Spray Characteristics of Pressure and Fine Mist Nozzles. *J. Tongji Univ. (Nat. Sci.)* **2005**, *33*, 1677–1679+1684.
31. Liang, P.; Zhou, H.P. Research on Prediction of Droplet Size Based on Grey Theory. *For. Mach. Woodwork. Equip.* **2008**, *8*, 54–56.
32. Guo, J.H.; Tan, X.S.; Bi, R.S. Model prediction and experiment study on spray droplet size distribution of pressure swirl nozzle. *Chem. Ind. Eng. Prog.* **2012**, *31*, 528–532.
33. Qu, R.J.; Ru, Y.; Lu, F. Experiment on speed and atomization performance of air rotary cage nozzle. *J. Jiangsu Univ. (Nat. Sci. Ed.)* **2020**, *41*, 452–458.
34. Ni, J.S.; Ru, Y.; Wang, J.S. Experimental Study on Prediction of Droplet Drift. *J. Agric. Mech. Res.* **2020**, *42*, 152–157.
35. Liu, R.H.; Wu, G.G.; Wang, P.F. Prediction model of mass median diameter of X-type swirl pressure nozzle. *J. Saf. Environ.* **2021**, *21*, 1467–1473.
36. Li, S.L.; Wu, G.G.; Wang, P.F.; Cui, Y.; Tian, C.; Han, H. A Mathematical Model for Predicting the Sauter Mean Diameter of Liquid-Medium Ultrasonic Atomizing Nozzle Based on Orthogonal Design. *Appl. Sci.* **2021**, *11*, 11628. [[CrossRef](#)]

Disclaimer/Publisher’s Note: The statements, opinions and data contained in all publications are solely those of the individual author(s) and contributor(s) and not of MDPI and/or the editor(s). MDPI and/or the editor(s) disclaim responsibility for any injury to people or property resulting from any ideas, methods, instructions or products referred to in the content.